



Decolourisation of Metanil Yellow by visible-light photocatalysis with N-doped TiO₂ nanoparticles: influence of system parameters and kinetic study

Dhruba Chakraborty, Susmita Sen Gupta*

Department of Chemistry, B N College, Dhubri, Assam, India
Tel. +91 9435561231; email: susmita2101@yahoo.co.in

Received 30 March 2013; Accepted 15 May 2013

ABSTRACT

A nitrogen-doped photocatalyst (N-TiO₂) is prepared from 15% TiCl₃ and 25% aqueous NH₃ solution as precursor. The synthesised material is characterised by XRD, BET, TEM, DRS and XPS and is used for photocatalytic decolourisation of Metanil Yellow under visible-light illumination. The experimental parameters, viz, photocatalyst dose, initial dye concentration and solution pH influence the decolourisation process. At pH 3.5, N-TiO₂ can decolourise almost 89% of the dye at equilibrium within 240 min. COD study reveals ~92% mineralisation of the dye in 360 min of irradiation. The photocatalytic reaction is allowed to proceed only after the attainment of adsorption equilibrium between N-TiO₂-Metanil Yellow. The adsorption is carried out by batch process under different experimental conditions, namely, N-TiO₂ dose, initial dye concentration and solution pH. The adsorption process attains equilibrium within 60 min and follows Lagergren first-order kinetics. On the other hand, the photocatalytic decolourisation of Metanil Yellow is suitably fitted with the modified Langmuir–Hinselwood model. Modification of TiO₂ improved the decolourisation of the dye by ~8 times compared to TiO₂ P25.

Keywords: Decolourisation; Kinetics; Metanil Yellow; Nitrogen-doped Titania; Photocatalysis

1. Introduction

Dyes are common constituents of effluents discharged by various industries, namely, leather, cosmetics, paper, printing, plastic, pharmaceuticals, food, etc. Colour in water is aesthetically unpleasant and may contain appreciable concentration of materials with high oxygen demand and suspended solids. Many dyes have toxic as well as carcinogenic, mutagenic and teratogenic effects [1] on aquatic life and human beings [2]. Moreover, coloured water has less

light penetrating power, which hinders photosynthesis in aquatic plants, adversely affects their growth and decreases the natural purification process. On the other hand, coloured effluents often contain a spectrum of heavy metals.

Metanil Yellow is a highly water-soluble dye having azo group. Skin contact of the dye causes allergic dermatitis [3]. On the other hand, methaemoglobinaemia is caused by oral exposure of the dye [4]. The intestinal and enzymic disorders in man by the consumption of Metanil Yellow have already been established [5,6]. Prasad and Rastogi [7] reported the

*Corresponding author.

possibility of haematological changes by this dye. The animal study indicates that chronic consumption of Metanil Yellow can predispose both the developing and the adult central nervous system [8]. The long-term chronic toxicosis of Metanil Yellow causing histopathological alterations in liver and kidney in albino rat indicates that the long-term use of this dye can harm human system, not only causing kidney and liver failure but sometimes it may also cause carcinoma.

Considering the toxic nature of dyes, various physical and chemical processes are tried by different group of workers for their removal, namely, nanofiltration [9–11], coagulation/flocculation [12], electro-coagulation [13,14] and electro-flocculation [15], ion-flotation [16], Fenton oxidation process [17–19], precipitation [20,21], adsorption [22–31], catalysis [32–35] and photo-catalysis [36–46], etc.

Out of all these techniques, the use of visible-light active photocatalyst for degradation of environmental pollutants has attracted considerable attention in last few years. Being the renewable source of energy, sunlight plays an important role in making the pollutant abatement processes cost-effective and sustainable. Titanium dioxide (TiO_2), a metal-oxide semiconductor, has been studied widely as a photocatalytic material [47] due to its high efficiency, low-cost, chemical inertness and photo-stability [48]. However, the use of TiO_2 as photocatalyst is limited by its wide band gap ($\sim 3.2\text{ eV}$ for anatase) allowing only a small fraction of the solar spectrum ($\sim 4\text{--}5\%$) to be absorbed in the photo-excitation process. Hence, some modifications are to be made so that TiO_2 can act as an effective visible-light photocatalyst. Doping of TiO_2 has been found to be a feasible approach for extending its light absorption into the visible region. The non-metal-doped TiO_2 has attracted considerable attention due to its photocatalytic activity in the visible-light region [49–55]. Among all these dopants, N has been found to be one of the most attractive and widely used anions for TiO_2 modification [56–61]. Both electronic and surface structure of TiO_2 can be changed by N-doping, the electronic structure determines the light response range and redox power of carriers while the surface structure controls surface transfer of carriers [62]. Asahi et al. [63] suggested that doping of N causes a band-gap narrowing by mixing of N 2p states with O 2p states. However, the observation of Irie et al. [64] did not support the narrowing of the band gap and suggested the formation of an isolated narrow band above the valence band, which is responsible for visible-light response of the photocatalyst.

Adsorption is one of the most important physico-chemical processes that occur at the solid-liquid and solid-gas interfaces. As photocatalytic decolourisation is accompanied by adsorption, the photocatalytic reaction is generally allowed to start after attainment of adsorption equilibrium in dark. In the present study, nano-sized ($\leq 10\text{ nm}$) N-doped TiO_2 was synthesised and characterised. The material was then used to decolourise Metanil Yellow dye in aqueous system under visible-light irradiation after attainment of adsorption equilibrium in dark. The percentage mineralisation of the dye was studied through Chemical Oxygen Demand (COD) measurement at different intervals of time.

2. Materials and methods

2.1. Materials

TiCl_3 (15%, Loba Chemie) and 25% NH_3 solution (E Merck) were used as sources of titanium and nitrogen, respectively. The TiO_2 P25 (AEROXIDE) was procured from Evonik (Degussa) Industries AG, Germany. Metanil Yellow [sodium salt of m-(p-anilinophenyl-azo) benzenesulphonic acid] (C.I. number: 13065, molecular formula: $\text{C}_{18}\text{H}_{14}\text{N}_3\text{NaO}_3\text{S}$) was procured from Loba-Chemie and was used without further purification. The structure of the dye is given in Fig. 1.

All other reagents were of analytical grade.

2.2. Preparation of the catalyst

150 ml of TiCl_3 was taken in a Teflon beaker and 100 ml aqueous NH_3 solution was added drop-wise with constant stirring at 353 K. The process took about 2 h, after which the mixture was stirred for an additional period of 1 h. The colour of the mixture first changed to blue and then became brownish-yellow. The solid precipitate was separated and washed with distilled water for several times and finally dried in air oven at 343 K. The sample was then calcined at 623 K for 4 h in a muffle furnace to get a yellowish-brown powder.

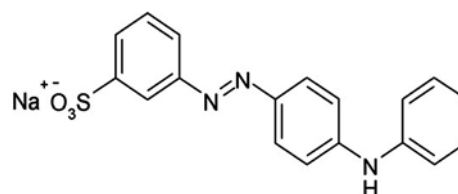


Fig. 1. Structure of Metanil Yellow.

2.3. Characterisation methods

The characterisation of the sample was done by taking XRD (Rigaku Miniflex diffractometer using nickel-filtered CuK α radiation), TEM (JEOL JEM 2100 instrument operating at an accelerating voltage of 200 kV), XPS (ThermoScientific ESCALAB 250 instrument with monochromatised Al X-ray source) and DRS (HITACHI-400 spectrophotometer). The BET surface area of the catalyst was measured by nitrogen adsorption method at 77 K with the help of Quantachrome Autosorb-1C surface area analyser, using BET equation.

2.4. Determination of adsorption efficiency

The adsorption of Metanil Yellow on N-TiO $_2$ was carried out in 100 ml Erlenmeyer flasks by mixing together a fixed amount of N-TiO $_2$ dose (0.50 g L $^{-1}$) with a constant volume of aqueous dye solution. The mixture in the flask was agitated by placing them in a constant-temperature water bath thermostat shaker for a known time interval under dark. It was then centrifuged (Remi R 24) and the concentration of dye solution remaining unadsorbed in the supernatant liquid was determined with spectrometer (Elico SL 177, India) at $\lambda_{\text{max}} = 502$ nm. The influences of N-TiO $_2$ load (0.25–2.0 g L $^{-1}$), initial dye concentration (18.0–36.0 $\mu\text{mol L}^{-1}$) and pH (3.5–11.0) on dye adsorption were studied.

2.5. Determination of photocatalytic activity

The catalytic reaction was carried out in a glass reactor having water circulation facility. A 250 W halogen bulb was used as the source of visible light fitted with a glass filter to cut-off short wavelengths ($\lambda < 420$ nm). The schematic diagram of the photocatalytic reactor is given in Fig. 2.

In a typical reaction, 200 ml (18 $\mu\text{mol L}^{-1}$) of the dye solution was taken with requisite amount of the catalyst and kept in dark for 60 min under stirring to attain the adsorption–desorption equilibrium. The mixture was then exposed to visible light under constant stirring with the help of a magnetic stirrer. The concentration of dye after adsorption (60 min) was considered as the initial concentration for photocatalytic study. Effluent was collected at a regular intervals and the concentration of the dye was measured with the help of a spectrometer as before.

2.6. Determination of percentage mineralisation

COD is an index of water pollution by organics and it is a parameter used for quality discharge. COD

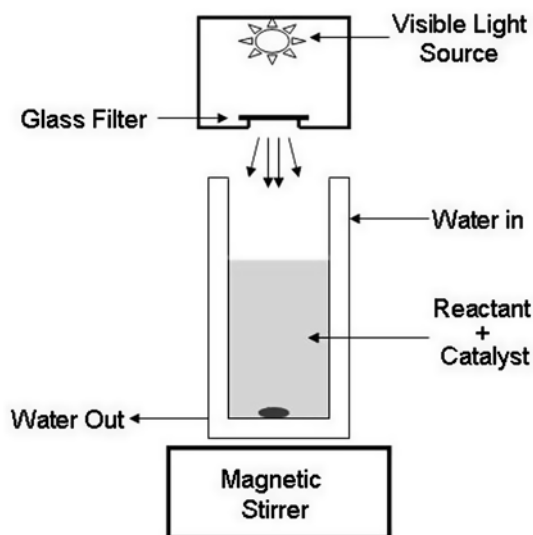


Fig. 2. Schematic diagram of the photocatalytic reactor.

differences with irradiation time are exclusively related to the degree of oxidation of the organic matter as a whole. The dichromate reflux method is used to estimate COD [65,66].

3. Results and discussion

3.1. Photocatalyst characterisation

The details of the characterisation of the nitrogen-doped titania catalyst, N-TiO $_2$, was published elsewhere [67]. The main features of the findings are listed below:

- X-ray powder diffraction showed that N-TiO $_2$ was in a highly crystalline anatase phase. The average particle size calculated on the basis of Scherrer equation was found to be approximately 6.2 nm.
- Diffuse reflectance UV–visible spectroscopy showed considerable absorption of radiation in the visible range that extends up to 600 nm. There was a red shift in the band gap energy in N-TiO $_2$ compared to undoped TiO $_2$. The narrower band gap was assumed to be responsible for relatively easier excitation of electron from the valence band to the conduction band in N-TiO $_2$, which in turn increases the photocatalytic activity of the material.
- The TEM images revealed the presence of agglomerates of primary particles with crystallite size ranging from about 6 to 10 nm.
- The surface area of N-TiO $_2$ determined with the help of BET method was found to be 176 m 2 /g.

- X-ray photoelectron spectroscopy of N-TiO₂ showed a binding energy peak at 400 eV, which was attributed to the presence of N1s electron in the sample in O–Ti–N environment.

3.2. Influence of experimental parameter on dye adsorption/ decolourisation

3.2.1. Influence of N-TiO₂ load on adsorption

The adsorption of Metanil Yellow was rapid on the onset of the process and the uptake of dye increased with the increase in the interaction time. The process attained equilibrium within 60 min. With initial dye concentration of 18.0 μmol L⁻¹, the uptake increased from 18.88 to 26.75% for N-TiO₂ dose of 0.25–1.5 g L⁻¹, although the amount of dye adsorbed per unit mass of N-TiO₂ decreased from 6.82 to 1.62 mg g⁻¹ for the same variation of N-TiO₂ dose. While the higher amount of titania provided more surface for the dye to get adsorbed on it, a large amount of adsorbent effectively reduces the unsaturation of the adsorption sites and, correspondingly, the number of such sites per unit mass comes down resulting in comparatively less adsorption at higher adsorbent amount [68]. Moreover, it was observed

that further increase of adsorbent dose (2.0 g L⁻¹) decreased the percentage adsorption to 21.78%, which may be due to particle agglomeration [69] (Table 1). Fig. 3 represents the % removal vs. time plots for different doses of N-TiO₂.

3.2.2. Influence of N-TiO₂ load on decolourisation

The decolourisation of the dye on different doses of N-TiO₂ is given in Fig. 4, where the equilibrium was attained within 240 min. The decolourisation of Metanil Yellow increased with the increase in N-TiO₂ loading from 0.25 g L⁻¹ (86.21% at 240 min) to 1.50 g L⁻¹ (96.96% at 240 min). However, a reverse trend was observed by increasing N-TiO₂ dose above 1.50 g L⁻¹ (for 2.0 g L⁻¹: 90.20% at 240 min) (initial dye concentration 18 μmol g L⁻¹, time 240 min; Table 1). This variation of dye decolourisation is observed in Fig. 5.

The result revealed that increase in the catalyst amount increased the decolourisation process, which was due to the larger amount of photo-electrons that accelerate the dye decolourisation [37]. On the other hand, the increase in the catalyst load beyond the optimum amount might result in the agglomeration of catalyst particles, making a part of the catalyst surface

Table 1
Influence of experimental parameters on extent of adsorption (%) and decolourisation (%) of Metanil Yellow on N-TiO₂

Parameters	Extent of adsorption (%)		Extent of decolourisation (%)		
	At 10 min	At 60 min	At 10 min	At 240 min	
	N-TiO ₂ dose (g L ⁻¹) (Initial dye concentration 18 μmol L ⁻¹ , pH 3.5)	0.25	15.93	18.88	3.25
	0.50	16.77	23.38	5.89	89.48
	0.75	18.21	24.07	8.33	91.70
	1.0	19.29	24.97	11.29	94.08
	1.25	20.49	26.24	28.45	95.76
	1.50	20.98	26.75	31.62	96.96
	1.75	19.02	25.24	24.25	93.87
	2.0	15.29	21.78	22.49	90.20
Initial dye concentration (μmol L ⁻¹) (N-TiO ₂ dose 0.50 g L ⁻¹ , pH 3.5)	18.0	16.77	23.38	5.89	89.48
	22.5	14.39	22.20	5.01	87.00
	27.0	14.01	21.10	4.98	85.80
	31.5	12.23	19.40	4.71	84.78
	36.0	10.77	18.10	4.00	82.90
pH (N-TiO ₂ dose 0.50 g L ⁻¹ , Initial dye concentration 18 μmol L ⁻¹)	3.5	16.77	23.38	5.89	89.48
	4.0	2.11	4.83	4.77	64.18
	4.5	1.11	4.11	3.59	23.50
	7.0	0.81	3.43	3.01	14.39
	9.0	0.73	2.74	2.49	6.86
	11.0	0.02	0.12	0.01	2.46

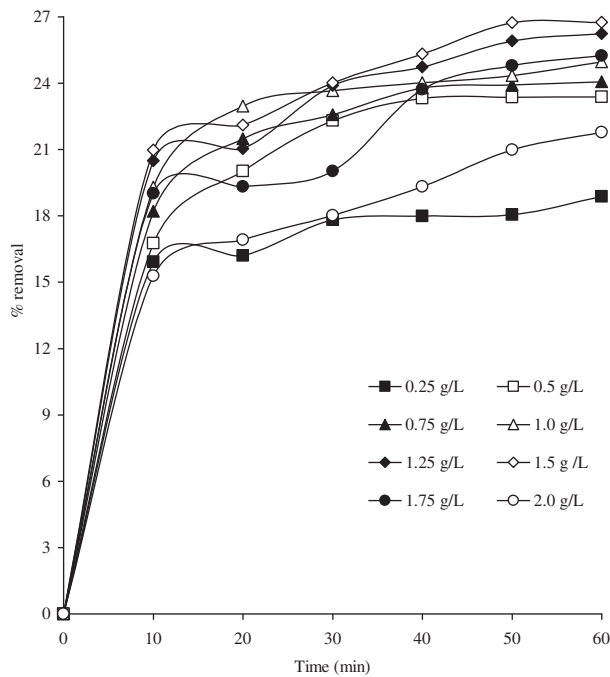


Fig. 3. Influence of N-TiO₂ dose on adsorption of Metanil Yellow at 303 K (initial dye concentration 18 $\mu\text{mol L}^{-1}$, pH 3.5).

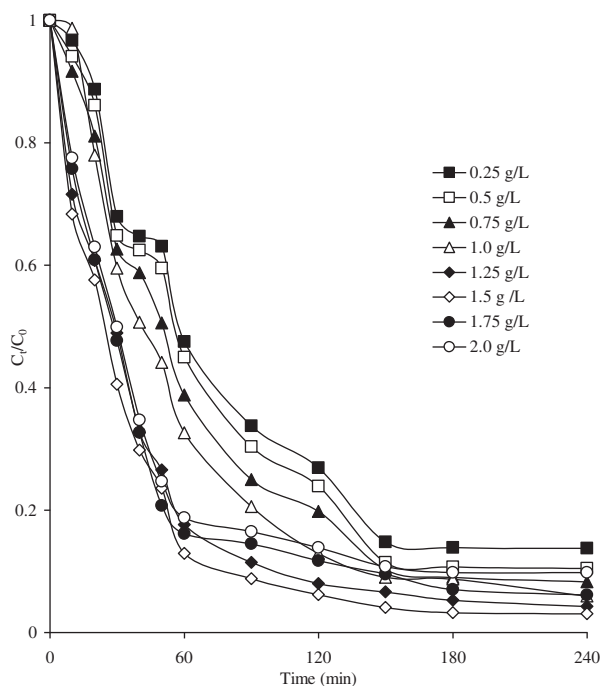


Fig. 4. Influence of N-TiO₂ dose on decolourisation of Metanil Yellow at 303 K (initial dye concentration 18 $\mu\text{mol L}^{-1}$, pH 3.5).

unavailable for light absorption, lowering the efficiency of decolourisation [70]. According to Sun et al. [71], the concentration of $\cdot\text{OH}$ radical, a primary oxidant in the photocatalytic system, decreases due to the obstruction offered to the incident light by the excess catalyst. This in turn decreased the efficiency of the dye decolourisation. Moreover, the rate of deactivation of activated molecules by collision with ground-state N-TiO₂ increases with the increase in the amount of N-TiO₂ in reaction medium, which reduces the site density for surface holes and electrons. This can also hinder the dye decolourisation process [72,73].

3.2.3. Influence of initial concentration of Metanil Yellow on adsorption

The extent of adsorption varies from 23.38 to 18.10% (4.23–5.33 mg g^{-1}) (Table 1) by increasing the initial concentration of dye from 18.0 to 36.0 $\mu\text{mol L}^{-1}$. Initial higher uptake was observed for first 10 min and equilibrium was attained within 60 min for all the cases (Fig. 6).

At low initial concentration of Metanil Yellow, the ratio of the number of dye molecules to the number of available adsorption sites was small and thus the

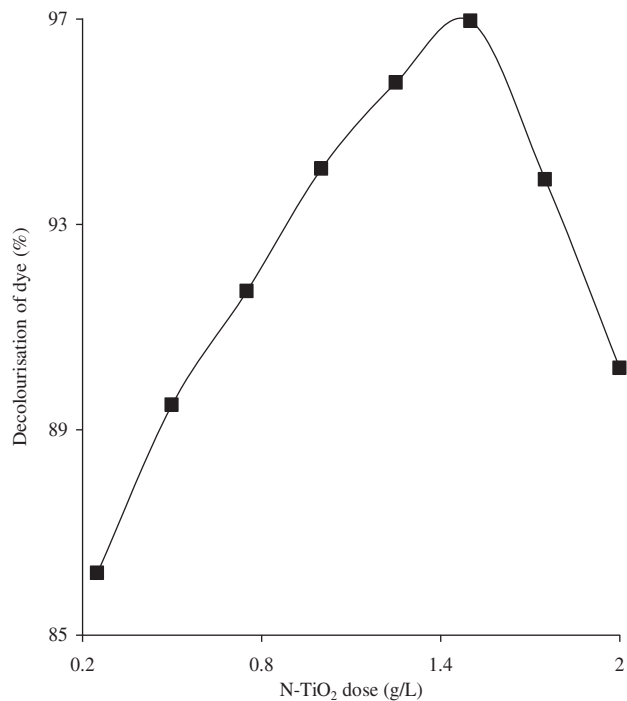


Fig. 5. Variation of maximum decolourisation of Metanil Yellow with N-TiO₂ dose at 240 min (initial dye concentration 18 $\mu\text{mol L}^{-1}$, pH 3.5).

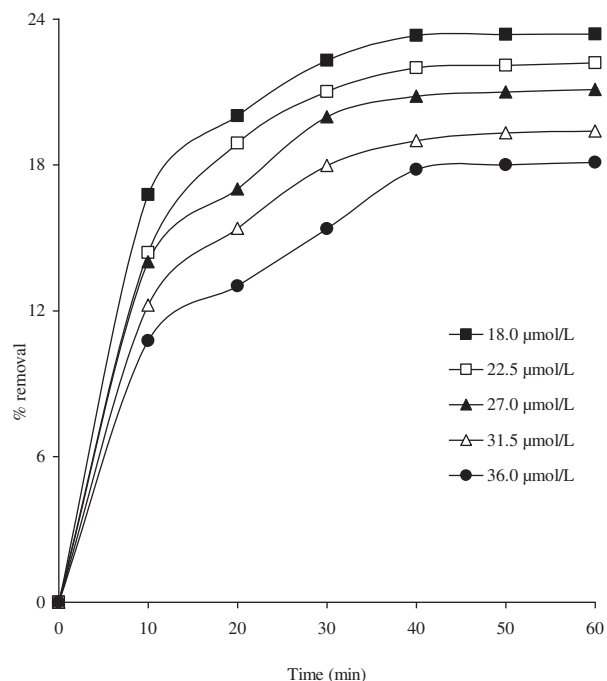


Fig. 6. Influence of initial dye concentration on adsorption of Metanil Yellow at 303 K (N-TiO₂ dose 0.5 g L⁻¹, pH 3.5).

adsorption was independent of the initial concentration, which depends on the driving force that was determined by the concentration gradient. At higher concentration of the dye, the active sites of the N-TiO₂ were surrounded by a large number of dye molecules and were likely to take up their full quota of dye molecules depending upon the degree of unsaturation [74].

3.2.4. Influence of initial concentration of Metanil Yellow on decolourisation

Fig. 7 shows the influence of initial concentration of dye on decolourisation process. The % decolourisation decreases from 89.48 to 82.90% on increasing the dye concentration from 18.0 to 36.0 μmol L⁻¹ (for N-TiO₂ 0.50 g L⁻¹, time 240 min; Table 1).

At high dye concentration, the active sites are covered by the dye molecules hindering the production of ·OH radicals on the surface of catalyst. Consequently, the photocatalytic decolourisation decreases as fewer ·OH radicals are available to oxidise large number of dye molecules [75]. On the other hand, Daud et al. [19] suggested that increase in the dye concentration allows more dye molecules to be scavenged by the same amount of ·OH generated, leading to a decrease in the decolourisation efficiency. Moreover, the reaction of Metanil Yellow can form some

intermediates that may interfere in the process. The increase of initial dye concentration may produce more intermediates, thus creating more competitions resulting in the decrease of decolourisation of dyes [76].

3.2.5. Influence of pH on adsorption

The adsorption of Metanil Yellow on N-TiO₂ was studied by varying the solution pH from 3.5 to 11.0 (Fig. 8). The uptake was maximum at pH 3.5 [23.38% (4.23 mg g⁻¹) at 240 min] and then went down with the increase in pH (Table 1).

At lower pH, the high electrostatic attraction between the positively charged surface of N-TiO₂ and anionic dye facilitates the adsorption process. As the solution pH increases, the surface charge turns towards negative and adsorption of dye anions comes down [77]. In an alkaline solution, there may be competition between OH⁻ ions and dye anions for negatively charged adsorption sites on the surface of the adsorbent and the adsorption of bulky dye anions get suppressed by the highly mobile OH⁻ ions.

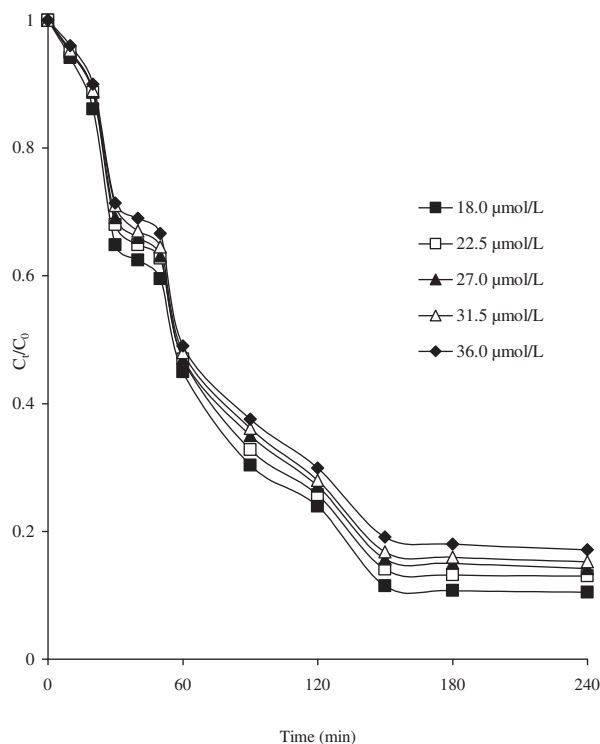


Fig. 7. Influence of initial dye concentration on decolourisation of Metanil Yellow at 303 K (N-TiO₂ dose 0.5 g L⁻¹, pH 3.5).

3.2.6. Influence of pH on decolourisation

The extent of decolourisation of dyes on N-TiO₂ was found to be more at lower pH and decreased with increase in pH (Fig. 9). At pH 3.5, 0.5 g L⁻¹ N-TiO₂ could decolourise 89.48% of Metanil Yellow (initial dye concentration 18 μmol L⁻¹) in 240 min. On the other hand, only 2.46% decolourisation was observed at pH 11.0 (Table 1).

The formation of the electrical double layer at the solid–electrolyte interface affects the sorption–desorption processes and thus separates the photogenerated electron–hole pairs on the surface of the semiconductor particles [78]. The ·OH radicals can be formed by the reaction between OH⁻ ions and positive holes. The positive holes are considered as the major oxidation species at low pH, whereas ·OH radicals are considered as predominant species at neutral or high pH levels. In alkaline medium, the coulombic repulsion between the negative-charged surface of photocatalyst and the OH⁻ ions prevents the formation of ·OH and thus decreases the photo-oxidation [78]. The adsorption of Metanil Yellow with sulphonate group favours at lower pH which might also have helped the decolourisation [76].

At pH 3.5, the decolourisation of Metanil Yellow on N-TiO₂ was almost six times higher compared to that at pH 7.0. A similar decolourisation trend over

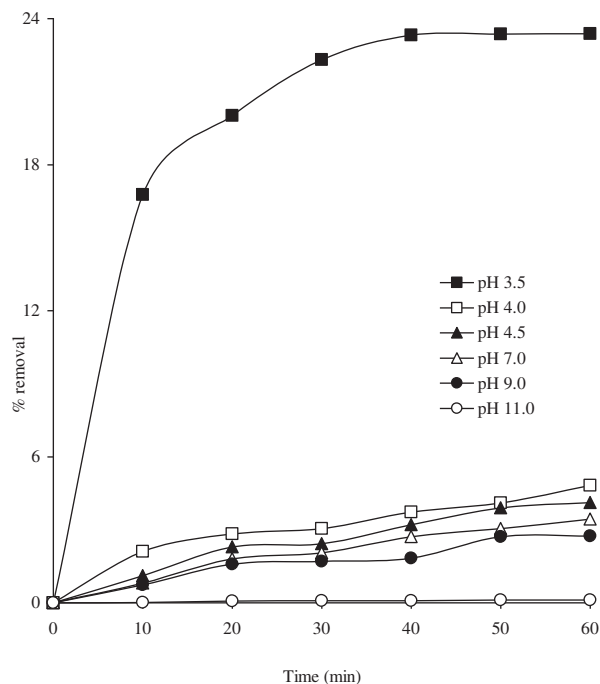


Fig. 8. Influence of solution pH on adsorption of Metanil Yellow at 303 K (N-TiO₂ dose 0.5 g L⁻¹, initial dye concentration 18 μmol L⁻¹).

TiO₂ photocatalyst under UV illumination was reported [76].

3.3. Kinetic study

3.3.1. Kinetics of adsorption

The adsorption of dye was studied by using Lagergren pseudo-first-order model [79,80],

$$\log(q_e - q_t) = \log q_e - k_1 t \quad (1)$$

where q_e and q_t are the amounts adsorbed per unit mass at equilibrium and at any time t and k_1 is the first-order adsorption rate constant. The $\log(q_e - q_t)$ vs. t plots (Fig. 10) are linear ($r \sim -0.92$ to -0.99) for all the experimental variables.

First-order rate constants increased from 3.63×10^{-2} to $12.20 \times 10^{-2} \text{ min}^{-1}$ for the N-TiO₂ dose varied from 0.25 to 1.50 g L⁻¹ and then again decreased to $4.88 \times 10^{-2} \text{ min}^{-1}$ for N-TiO₂ 2.0 g L⁻¹. Similarly, the k_1 values were in the range of 9.19×10^{-2} to $4.92 \times 10^{-2} \text{ min}^{-1}$ for the variation of initial dye concentration from 18 to 36.0 μmol L⁻¹ and 9.19×10^{-2} to $1.01 \times 10^{-2} \text{ min}^{-1}$ as the solution pH changed from 3.5 to 11.0. All k_1 values are listed in Table 2.

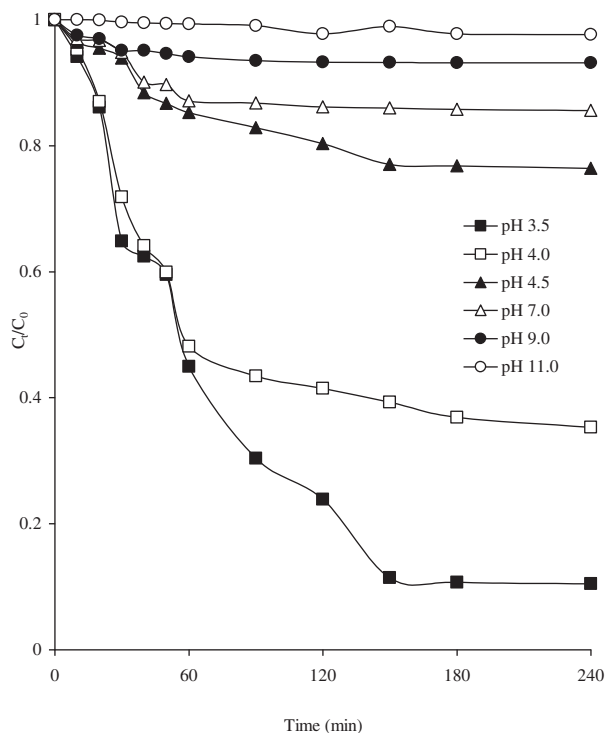


Fig. 9. Influence of solution pH on decolourisation of Metanil Yellow on N-TiO₂ at 303 K (N-TiO₂ dose 0.5 g L⁻¹, initial dye concentration 18 μmol L⁻¹).

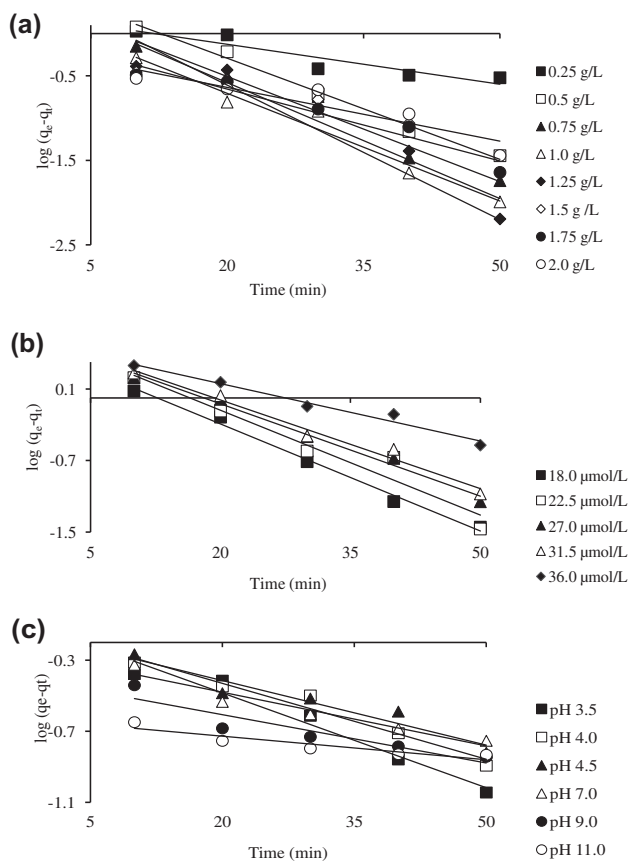


Fig. 10. Lagergren plots for adsorption of Metanil Yellow on N-TiO₂ for variation of (a) N-TiO₂ dose (b) initial dye concentration and (c) solution pH.

3.3.2. Kinetics of decolourisation

The kinetics of Metanil Yellow decolourisation on N-TiO₂ was studied by modified Langmuir–Hinshelwood (L–H) mechanism, given by,

$$-dc/dt = (kK_e C)/(1 + K_e C) \quad (2)$$

where C is the concentration of dye, k is the apparent reaction rate constant (min^{-1}), K_e is the apparent equilibrium constant for the adsorption of the dye on the catalyst surface.

Eq. (2) can be written as,

$$t = 1/(K_e k) \ln(C_0/C_t) + (1/k)(C_0 - C_t) \quad (3)$$

where C_0 and C_t are the concentration of dye at initial and at any time t , respectively.

For the sufficient low concentration of dye, Eq. (4) can be expressed as,

$$\ln(C_0/C_t) = kK_e t = kt' \quad (4)$$

Table 2

Lagergren first order rate constants (for dye adsorption) and Langmuir–Hinshelwood first order rate constants (for dye decolourisation) on N-TiO₂

Parameters	Lagergren rate constants $k_1 \times 10^2$ (min^{-1})	Langmuir–Hinshelwood rate constants $k' \times 10^3$ (min^{-1})
N-TiO ₂ dose (g L^{-1})	0.25	3.63
(Initial dye concentration $18 \mu\text{mol L}^{-1}$, pH 3.5)	0.75	9.7
	0.50	3.63
	0.75	9.19
	1.00	9.53
	1.25	9.78
	1.50	10.52
	1.75	12.20
	2.00	6.54
Initial dye concentration ($\mu\text{mol L}^{-1}$) (N-TiO ₂ dose 0.50 g L^{-1} , pH 3.5)	18.0	4.88
	22.5	9.19
	27.0	8.98
	31.5	7.92
	36.0	7.59
	4.92	8.5
pH (N-TiO ₂ dose 0.50 g L^{-1} , Initial dye concentration $18 \mu\text{mol L}^{-1}$)	3.5	9.19
	4.0	3.24
	4.5	2.78
	7.0	2.32
	9.0	2.09
	11.0	1.01
	1.01	1.0

where kt' is the overall rate constant (min^{-1}). By plotting $\ln(C_0/C_t)$ as a function of irradiation time through regression, we obtained for each catalyst sample the kt' (min^{-1}) constant from the slopes.

The overall rate constant for dye–N-TiO₂ interactions was studied for the variation of catalyst load, initial dye concentration and solution pH. All the plots can be roughly considered as straight line (Fig. 11). Although the curves did not pass through the origin as required by the model, the intercepts were close to zero (varied from -0.001 to $+0.659$).

The kinetic study revealed that the decolourisation rates depend on the catalyst amount.

The rate constant increased from $9.7 \times 10^{-3} \text{ min}^{-1}$ to $14.68 \times 10^{-3} \text{ min}^{-1}$ when the catalyst load was increased from 0.25 g L^{-1} to 1.50 g L^{-1} . When the catalyst load was further increased to 2.0 g L^{-1} , the rate constant decreased to $9.0 \times 10^{-3} \text{ min}^{-1}$. Similarly, the rate constants decreased from 11.0×10^{-3} to $8.5 \times 10^{-3} \text{ min}^{-1}$ as concentration of Metanil Yellow was increased from 18.0 to $36.0 \mu\text{mol L}^{-1}$. These results were consistent with the influence of variation in dye

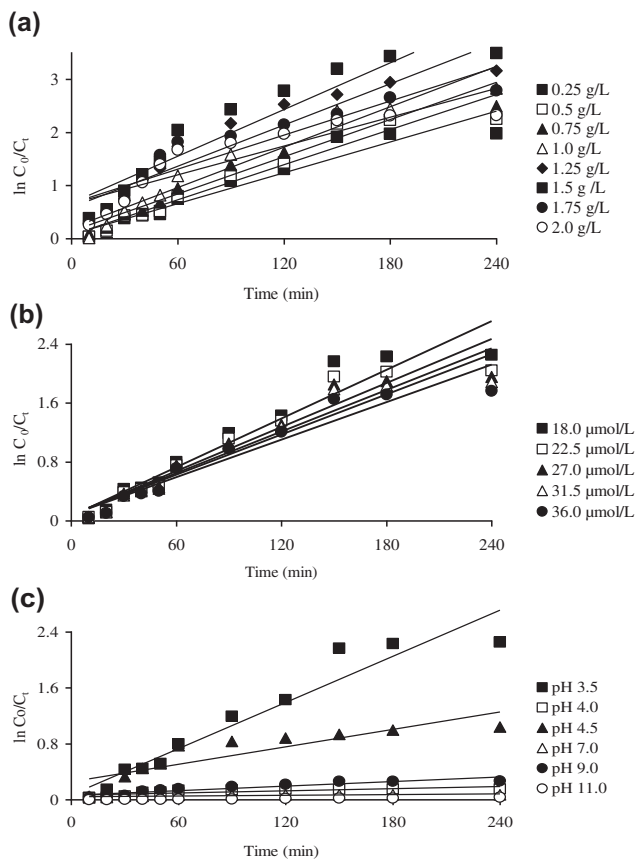


Fig. 11. Langmuir-Hinselwood plots for Metanil Yellow degradation on N-TiO₂ for the variation of (a) N-TiO₂ dose (b) initial dye concentration and (c) solution pH.

concentration on photocatalytic decolourisation. It was observed that the decolourisation rates were pH dependent and lower pH favoured the process more efficiently as was evident from the overall rate constant calculated at different pH levels: $kt'_{\text{pH } 3.5}$ (11.0×10^{-3}) $> kt'_{\text{pH } 4.0}$ (5.0×10^{-3}) $> kt'_{\text{pH } 4.5}$ (4.2×10^{-3}) $> kt'_{\text{pH } 7.0}$ (2.0×10^{-3}) $> kt'_{\text{pH } 9.0}$ (1.1×10^{-3}) $> kt'_{\text{pH } 11.0}$ (1.0×10^{-3}). All k' values are given in the Table 2.

3.4. Adsorption isotherms

The adsorption capacities of undoped TiO₂ and N-TiO₂ was studied by the well-known Langmuir isotherm [81] given by,

$$C_e/q_e = (1/bq_m) + (1/q_m)C_e \quad (5)$$

where C_e = concentration of dye at equilibrium, q_e = amount of dye adsorbed per unit mass of adsorbent at equilibrium, q_m = Langmuir monolayer adsorption capacity.

The linear Langmuir plots were obtained by plotting C_e/q_e vs. C_e ($r \sim 0.97$). The q_m values were calculated as 2.79×10^{-4} and $1.84 \times 10^{-3} \text{ mg g}^{-1}$ for pure P25 and modified TiO₂, respectively, indicating that N-TiO₂ was much better adsorbent for Metanil Yellow than TiO₂ P25.

3.5. A comparative study of decolourisation of Metanil Yellow on N-TiO₂ and pure TiO₂ P25

The decolourisation of Metanil Yellow by N-TiO₂ was compared with pure TiO₂ P25. Fig. 12 reveals that at equilibrium time of 240 min, 0.5 g L^{-1} of N-TiO₂ could decolourise $\sim 89.48\%$ of dye from an initial dye concentration of $18 \mu\text{mol L}^{-1}$. Under the same experimental conditions, only 10.98% dye decolourisation was observed in presence of undoped TiO₂. The results show that the modified TiO₂ can decolourise Metanil Yellow ~ 8 times more than pure TiO₂ P25. In the blank experiment (carried out with the dye in absence of catalyst under visible light), only 2.56% decolourisation was observed in 240 min of irradiation (Fig. 12). Besides this, the Langmuir-Hinselwood rate constant of Metanil Yellow decolourisation by N-TiO₂ was found to be 55 times higher compared to the rate constant of the dye decolourisation by undoped TiO₂

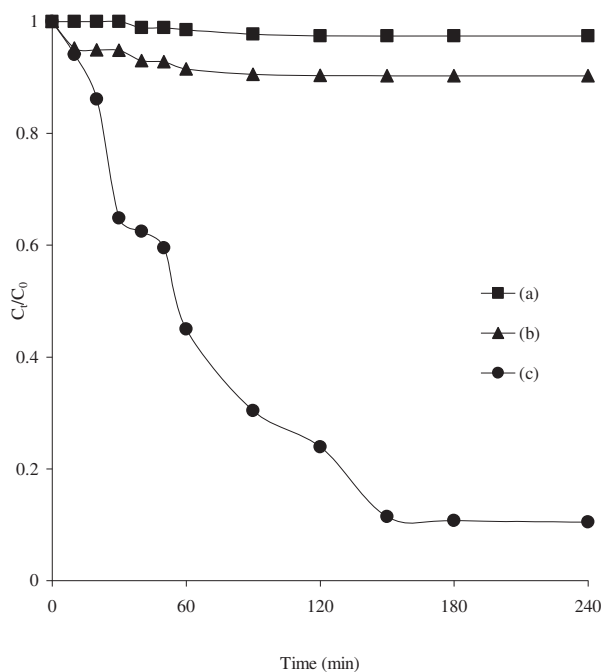


Fig. 12. Comparison of the photocatalytic decolourisation of Metanil Yellow (a) blank (b) TiO₂ P25 (c) N-TiO₂ (initial dye concentration $18.0 \mu\text{mol L}^{-1}$, N-TiO₂ dose 0.5 g L^{-1} , temperature 303 K).

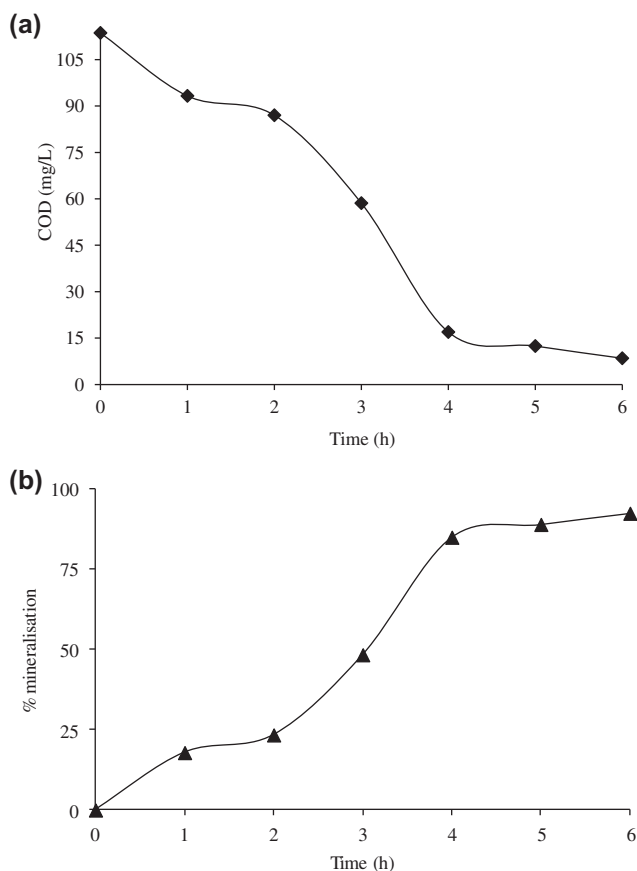


Fig. 13. (a) Variation of COD with irradiation time (b) Variation of percentage mineralisation with irradiation time (Initial dye concentration $18.0 \mu\text{mol L}^{-1}$, N-TiO₂ dose 0.5 g L^{-1} , temperature 303 K).

under similar experimental conditions (k_t' for N-TiO₂: $11.0 \times 10^{-3} \text{ min}^{-1}$; TiO₂ P25: $2.0 \times 10^{-4} \text{ min}^{-1}$).

3.6. Mineralisation studies of dyes

The reduction of COD reflects the extent of degradation or mineralisation of an organic species. In this study, for Metanil Yellow (Initial concentration of dye $18.0 \mu\text{mol L}^{-1}$, catalyst load 0.5 g L^{-1}), a steady decrease in COD with the increase in the irradiation time was observed (Fig. 13). In one hour of irradiation, the percentage mineralisation was found to be 17.91% and it went up to 92.54% in 6 h. It was observed that the percentage decolourisation was more than the percentage mineralisation. While the reduction in COD in four hours of irradiation time was 85.07%, the percent decolourisation for the same period of time was 89.48%. This might be due to the formation of smaller uncoloured products, which contribute to the COD but did not impart any colour.

4. Conclusions

The photocatalytic decolourisation of Metanil Yellow was studied using N-doped TiO₂ as catalysts, synthesised by a very simple method using TiCl₃ and aqueous NH₃. The results of the study can be summarised as follows:

- (1) Adsorption of Metanil Yellow was influenced by N-TiO₂ dose, initial dye concentration and solution pH.
- (2) The experimental variables (N-TiO₂ dose, initial dye concentration and solution pH) also influenced the dye decolourisation process.
- (3) The decolourisation efficiency increased with the increase in N-TiO₂ load from 0.25 to 1.50 g L^{-1} and then again decreased when the load was increased to 2.0 g L^{-1} . The decrease in initial dye concentration enhanced the decolourisation process. Moreover, the acidic pH favoured the decolourisation of dye compared to neutral and alkaline pH.
- (4) Adsorption interactions followed Lagergren first-order kinetic model.
- (5) The photo-catalytic decolourisation of dye followed first-order kinetics, which fitted the modified Langmuir–Hinshelwood model.
- (6) Parameters, such as N-TiO₂ dose, initial dye concentration and solution pH played an important role affecting the reaction rate constants for both the processes, i.e. adsorption as well as decolourisation.
- (7) Adsorption isotherm for N-TiO₂ was much higher compared to undoped TiO₂ P25.
- (8) Modification of TiO₂ improved the decolourisation compared to TiO₂ P25. The N-TiO₂ decolourised the dye almost eight times more compared to TiO₂ P25.
- (9) The percentage mineralisation of the dye was found to be 17.91% in one hour and it went up to 92.54% in six hours.

Acknowledgements

The authors are thankful to Dr. C.V.V. Satyanarayana, Scientist, Heterogeneous Catalysis Division, NCL, Pune for his support in various stages of this work. We gratefully acknowledge the use of CAMCOR facilities of University of Oregon, USA, which have been purchased with combination of federal and state funding. The authors are also thankful to U.G.C, New Delhi for financial assistance through a Major Research Project grant.

References

- [1] G. McKay, M.S. Otterburn, D.A. Aga, Fuller's earth and fired clay as adsorbent for dye stuffs, *Equilibrium and rate constants*, *Water Air Soil Pollut.* 24 (1985) 307–322.
- [2] A.R. Gregory, S. Elliot, P. Kluge, Ames testing of Direct Black 3B parallel carcinogenicity, *J. Appl. Toxicol.* 1 (1991) 308–313.
- [3] B.M. Hausen, A case of allergic contact dermatitis due to Metanil Yellow, *Contact dermatitis* 31 (1994) 117–118.
- [4] S.M. Sachdeva, K.V. Mani, S.K. Adval, V.P. Jalpota, K.C. Rasela, D.S. Chadha, Acquired toxic methaemoglobinaemia, *J. Assoc. Physicians India* 40 (1992) 239–240.
- [5] M. Das, S. Ramchandani, R.K. Upreti, S.K. Khanna, Metanil Yellow: A biofunctional inducer of hepatic phase I and phase II xenoblastic-metabolising enzymes, *Food Chem. Toxicol.* 35 (1997) 835–838.
- [6] S. Ramchandani, M. Das, A. Joshi, S.K. Khanna, Effect of oral and parental administration of Metanil Yellow on some hepatic and intestinal biochemical parameters, *J. Appl. Toxicol.* 17 (1997) 85–91.
- [7] O.M. Prasad, P.B. Rastogi, Haematological changes induced by feeding common food colour, Metanil Yellow in albino mice, *Toxicol. Lett.* 16 (1983) 103–107.
- [8] T.N. Nagaraja, T. Desiraju, Effects of chronic consumption of Metanil Yellow by developing and adult rats on brain regional levels of noradrenaline, dopamine and serotonin, on acetylcholine esterase activity and on operant conditioning, *Food Chem. Toxicol.* 31 (1993) 41–44.
- [9] S. Cheng, D.L. Oatley, P.M. Williams, C.J. Wrigh, Characterisation and application of a novel positively charged nanofiltration membrane for the treatment of textile industry wastewaters, *Water Res.* 46 (2012) 33–42.
- [10] E. Ellouze, N. Tahri, R.B. Amar, Enhancement of textile wastewater treatment process using nanofiltration, *Desalination* 286 (2012) 16–23.
- [11] S. Yu, Z. Chen, Q. Cheng, Z. Lü, M. Liu, Application of thin-film composite hollow fiber membrane to submerged nanofiltration of anionic dye aqueous solutions, *Sep. Purif. Technol.* 88 (2012) 121–129.
- [12] M. Riera-Torres, C. Gutiérrez-Bouzán, M. Crespi, Combination of coagulation-foculation and nanofiltration techniques for dye removal and water reuse in textile effluents, *Desalination* 252 (2010) 53–59.
- [13] F. Zidane, P. Drogui, B. Lekhlif, J. Bensaid, J.-F. Blais, S. Belcadi, K. El kacem, Decolorization of dye-containing effluent using mineral coagulants produced by electrocoagulation, *J. Hazard. Mater.* 155 (2008) 153–163.
- [14] M.-C. Wei, K.-S. Wang, C.-L. Huang, C.-W. Chiang, T.-J. Chang, S.-S. Lee, S.-H. Chang, Improvement of textile dye removal by electrocoagulation with low-cost steel wool cathode reactor, *Chem. Eng. J.* 192 (2012) 37–44.
- [15] G. Ciardelli, N. Ranieri, The treatment and reuse of wastewater in the textile industry by means of ozonation and electro-flocculation, *Water Res.* 35 (2001) 567–572.
- [16] K. Shakir, A.F. Elkafrawy, H.F. Ghoneimy, S.G.E. Beheir, M. Refaat, Removal of Rhodamine B (a basic dye) and Thoron (an acidic dye) from dilute aqueous solutions and wastewater simulants by ion flotation, *Water Res.* 44 (2010) 1449–1461.
- [17] S. Meriç, H. Selcuk, M. Gallo, V. Belgiorno, Decolourisation and detoxifying of Remazol Red dye and its mixture using Fenton's reagent, *Desalination* 173 (2005) 239–248.
- [18] C.S.D. Rodrigues, L.M. Madeira, R.A.R. Boaventura, Optimization of the azo dye Procion Red H-EXL degradation by Fenton's reagent using experimental design, *J. Hazard. Mater.* 164 (2009) 987–994.
- [19] N.K. Daud, U.G. Akpan, B.H. Hameed, Decolorization of Sunzol Black DN conc. in aqueous solution by Fenton oxidation process: Effect of system parameters and kinetic study, *Desalin. Water Treat.* 37 (2012) 1–7.
- [20] M.-X. Zhu, L. Lee, H.-H. Wang, Z. Wang, Removal of an anionic dye by adsorption/precipitation processes using alkaline white mud, *J. Hazard. Mater.* 149 (2007) 735–741.
- [21] N.M. Mahmoodi, Photocatalytic ozonation of dyes using copper ferrite nanoparticle prepared by co-precipitation method, *Desalination* 279 (2011) 332–337.
- [22] A. Mittal, V.K. Gupta, A. Malviya, J. Mittal, Process development for the batch and bulk removal and recovery of a hazardous, water-soluble azo dye (Metanil Yellow) by adsorption over waste materials (Bottom Ash and De-oiled Soya), *J. Hazard. Mater.* 151 (2008) 821–832.
- [23] A. Mittal, V. Gajbe, J. Mittal, Removal and recovery of hazardous triphenylmethane dye, Methyl Violet through adsorption over granulated waste materials, *J. Hazard. Mater.* 150 (2008) 364–375.
- [24] R. Han, J. Zhang, P. Han, Y. Wang, Z. Zhao, M. Tang, Study of equilibrium, kinetic and thermodynamic parameters about Methylene Blue adsorption onto natural zeolite, *Chem. Eng. J.* 145 (2009) 496–504.
- [25] Z. Hu, H. Chen, F. Ji, S. Yuan, Removal of Congo Red from aqueous solution by cattail root, *J. Hazard. Mater.* 173 (2010) 292–297.
- [26] A. Mittal, V.K. Gupta, Adsorptive removal and recovery of the azo dye Eriochrome Black T, *Toxicol. Environ. Chem.* 92 (2010) 1813–1823.
- [27] C. Xia, Y. Jing, Y. Jia, D. Yue, J. Ma, X. Yin, Adsorption properties of Congo Red from aqueous solution on modified hectrite: Kinetic and thermodynamic studies, *Desalination* 265 (2011) 81–87.
- [28] M. Auta, B.H. Hameed, Modified mesoporous clay adsorbent for adsorption isotherm and kinetics of Methylene Blue, *Chem. Eng. J.* 198–199 (2012) 219–227.
- [29] L. Wang, L. Jian, Adsorption of C.I. Reactive Red 228 dye from aqueous solution by modified cellulose from flax shive: Kinetics, equilibrium, and thermodynamics, *Ind. Crops Prod.* 42 (2013) 153–158.
- [30] A. Mittal, D. Jhare, J. Mittal, Adsorption of hazardous dye Eosin Yellow from aqueous solution onto waste material De-oiled Soya: Isotherm, kinetics and bulk removal, *J. Mol. Liq.* 179 (2013) 133–140.
- [31] A. Mittal, V. Thakur, V. Gajbe, Adsorptive removal of toxic azo dye Amido Black 10B by hen feather, *Environ. Sci. Pollut. Res.* 20 (2013) 260–269.
- [32] W. Li, S. Zhao, B. Qi, Y. Du, X. Wang, M. Huo, Fast catalytic degradation of organic dye with air and MoO₃/Ce nanofibers under room condition, *Appl. Catal., B* 92 (2009) 333–340.
- [33] Y. Zhan, X. Zhou, B. Fu, Y. Chen, Catalytic wet peroxide oxidation of azo dye (Direct Blue 15) using solvothermally synthesized copper hydroxide nitrate as catalyst, *J. Hazard. Mater.* 187 (2011) 348–354.
- [34] R. Prihod'ko, I. Stolyarova, G. Gündüz, O. Taran, S. Yashnik, V. Parmon, V. Goncharuk, Fe-exchanged zeolites as materials for catalytic wet peroxide oxidation. Degradation of Rodamine G dye, *Appl. Catal., B* 104 (2011) 201–210.
- [35] A. Safavi, S. Momeni, Highly efficient degradation of azo dyes by palladium/hydroxyapatite/Fe₃O₄ nanocatalyst, *J. Hazard. Mater.* 201–202 (2012) 125–131.
- [36] K. Nagaveni, G. Sivalingam, M.S. Hegde, G. Madras, Solar photocatalytic degradation of dyes: high activity of combustion synthesized nano TiO₂, *Appl. Catal., B* 48 (2004) 83–93.
- [37] E. Bizani, K. Fytianos, I. Poullos, V. Tsidiris, Photocatalytic decolorization and degradation of dye solutions and wastewaters in the presence of titanium dioxide, *J. Hazard. Mater.* 136 (2006) 85–94.
- [38] K. Sahel, N. Perol, H. Chermette, C. Bordes, Z. Derriche, C. Guillard, Photocatalytic decolorization of Remazol Black 5 (RB5) and Procion Red MX-5B isotherm of adsorption, kinetic of decolorization and mineralization, *Appl. Catal., B* 77 (2007) 100–109.

- [39] V. Elías, E. Vaschetto, K. Sapag, M. Oliva, S. Casuscelli, G. Eime, MCM-41-based materials for the photo-catalytic degradation of Acid Orange 7, *Catal. Today* 172 (2011) 58–65.
- [40] A. Nezamzadeh-Ejehie, Z. Banan, A comparison between the efficiency of CdS nanoparticles/zeolite A and CdO/zeolite A as catalysts in photodecolorization of Crystal Violet, *Desalination* 279 (2011) 146–151.
- [41] S.K. Maji, A.K. Dutta, D.N. Srivastava, P. Paul, A. Mondal, B. Adhikary, Effective photocatalytic degradation of organic pollutant by ZnS nanocrystals synthesized via thermal decomposition of single-source precursor, *Polyhedron* 30 (2011) 2493–2498.
- [42] R.K. Upadhyay, M. Sharma, D.K. Singh, S.S. Amritphale, N. Chandra, Photo degradation of synthetic dyes using cadmium sulfide nanoparticles synthesized in the presence of different capping agents, *Sep. Purif. Technol.* 88 (2012) 39–45.
- [43] M. Sharma, T. Jain, S. Singh, O.P. Pandey, Photocatalytic degradation of organic dyes under UV–visible light using capped ZnS nanoparticles, *Sol. Energy* 86 (2012) 626–633.
- [44] X. Li, J. Zhu, L. Hexing, Comparative study on the mechanism in photocatalytic degradation of different-type organic dyes on SnS₂ and CdS, *Appl. Catal., B* 123–124 (2012) 174–181.
- [45] V.K. Gupta, R. Jain, A. Mittal, T.A. Saleh, A. Nayak, S. Agarwal, S. Sikarwar, Photo-catalytic degradation of toxic dye amaranth on TiO₂/UV in aqueous suspensions, *Mat. Sci. Eng. C* 32 (2012) 12–17.
- [46] J. Yang, J. Dai, J. Li, Visible-light-induced photocatalytic reduction of Cr(VI) with coupled Bi₂O₃/TiO₂ photocatalyst and the synergistic bisphenol A oxidation, *Environ. Sci. Pollut. Res.* 20 (2013) 2435–2447.
- [47] A. Fujishima, K. Hashimoto, T. Watanabe, *TiO₂ Photocatalysis: Fundamentals and Applications*, BKC, Tokyo, 1999.
- [48] C. Burda, Y. Lou, X. Chen, A.C.S. Samia, J. Stout, J.L. Gole, Enhanced nitrogen doping in TiO₂ nanoparticles, *Nano Lett.* 3 (2003) 1049–1051.
- [49] G. Liu, Z. Chen, C. Dong, Visible light photocatalyst: Iodine-doped mesoporous titania with a bicrystalline framework, *J. Phys. Chem. B* 110 (2006) 20823–20828.
- [50] W. Ren, Z. Ai, F. Jia, L. Zhang, X. Fan, Z. Zou, Low temperature preparation and visible light photocatalytic activity of mesoporous carbon-doped crystalline TiO₂, *Appl. Catal., B* 69 (2007) 138–144.
- [51] L. Lin, W. Lin, J.L. Xie, Y.X. Zhu, B.Y. Zhao, Y.C. Xie, Photocatalytic properties of phosphor-doped titania nanoparticles, *Appl. Catal., B* 75 (2007) 52–58.
- [52] L. Mai, C. Huang, D. Wang, Z. Zhang, Y. Wang, Effect of C doping on the structural and optical properties of sol-gel TiO₂ thin films, *Appl. Surf. Sci.* 255 (2009) 9285–9289.
- [53] H. Znad, Y. Kawase, Synthesis and characterization of S-doped Degussa P25 with application in decolorization of Orange II dye as a model substrate, *J. Mol. Catal. A* 314 (2009) 55–62.
- [54] M. Behpour, V. Atouf, Study of the photocatalytic activity of nanocrystalline S, N-codoped TiO₂ thin films and powders under visible and sun light irradiation, *Appl. Surf. Sci.* 258 (2012) 6595–6601.
- [55] X.-X. Zou, G.-D. Li, J. Zhao, J. Su, X. Wei, K.-X. Wang, Y.-N. Wang, J.-S. Chen, Light-driven preparation, microstructure, and visible-light photocatalytic property of porous carbon-doped TiO₂, *Int. J. Photoenergy* 2012 (2012) 1–9, doi: 10.1155/2012/720183.
- [56] J. Wang, W. Zhu, Y. Zhang, S. Liu, An efficient two-step technique for nitrogen-doped titanium dioxide synthesizing: Visible-light-induced photodecomposition of Methylene Blue, *J. Phys. Chem. C* 111 (2007) 1010–1014.
- [57] G.-S. Shao, X.-J. Zhang, Z.-Y. Yuan, Preparation and photocatalytic activity of hierarchically mesoporous-macroporous TiO_{2-x}N_x, *Appl. Catal., B* 82 (2008) 208–218.
- [58] J.-H. Xu, W.-L. Dai, J. Li, Y. Cao, H. Li, H. He, K. Fan, Simple fabrication of thermally stable apertured N-doped TiO₂ microtubes as a highly efficient photocatalyst under visible light irradiation, *Catal. Commun.* 9 (2008) 146–152.
- [59] Z. He, H.Y. He, Synthesis and photocatalytic property of N-doped TiO₂ nanorods and nanotubes with high nitrogen content, *Appl. Surf. Sci.* 258 (2011) 972–976.
- [60] Y. Wang, C. Feng, M. Zhang, J. Yang, Z. Zhang, Visible light active N-doped TiO₂ prepared from different precursors: origin of the visible light absorption and photoactivity, *Appl. Catal., B* 104 (2011) 268–274.
- [61] G.C. Collazzo, E.L. Foletto, S.L. Jahn, M.A. Villetti, Degradation of Direct Black 38 dye under visible light and sunlight irradiation by N-doped anatase TiO₂ as photocatalyst, *J. Environ. Manage.* 98 (2012) 107–111.
- [62] G. Liu, X. Wang, Z. Chen, H.-M. Cheng, G.Q.M. Lu, The role of crystal phase in determining photocatalytic activity of nitrogen doped TiO₂, *J. Colloid Interface Sci.* 329 (2009) 331–338.
- [63] R. Asahi, T. Morikawa, T. Ohwaki, K. Aoki, Y. Taga, Visible-light photocatalysis in nitrogen-doped titanium oxides, *Science* 293 (2001) 269–271.
- [64] H. Irie, Y. Watanabe, K. Hashimoto, Nitrogen-concentration dependence on photocatalytic activity of TiO_{2-x}N_x powders, *J. Phys. Chem. B* 107 (2003) 5483–5486.
- [65] APHA, *Standard Methods for the Examination of Water and Wastewater*, America Water Works Association, New York, 1999.
- [66] N.P. Tantak, S. Chaudhari, Degradation of azo dyes by sequential Fenton's oxidation and aerobic biological treatment, *J. Hazard. Mater.* B136 (2006) 698–705.
- [67] D. Chakraborty, S. Sen Gupta, Photo-catalytic decolorization of toxic dye with N-doped titania: A case study with Acid Blue 25, *J. Environ. Sci.* 25 (2013) 1034–1043, doi: 10.1016/S1001-0742(12)60108-9.
- [68] K.G. Bhattacharyya, S. Sen Gupta, Adsorptive accumulation of Cd(II), Co(II), Cu(II), Pb(II), and Ni(II) from water on montmorillonite: Influence of acid activation, *J. Colloid Interface Sci.* 310 (2007) 411–424.
- [69] S.A. Simakov, Y. Tsur, Surface stabilization of nano-sized titanium dioxide: Improving the colloidal stability and the sintering morphology, *J. Nanopart. Res.* 9 (2007) 403–417.
- [70] M. Huang, C. Xu, Z. Wu, Y. Huang, J. Lin, J. Wu, Photocatalytic discolorization of Methyl Orange solution by Pt modified TiO₂ loaded on natural zeolite, *Dyes Pigm.* 77 (2008) 327–334.
- [71] J. Sun, L. Qiao, S. Sun, G. Wang, Photocatalytic degradation of Orange G on nitrogen-doped TiO₂ catalysts under visible light and sunlight irradiation, *J. Hazard. Mater.* 155 (2008) 312–319.
- [72] L.C. Chen, T.C. Chou, Photobleaching of Methyl Orange in titanium dioxide suspended in aqueous solution, *J. Mol. Catal.* 85 (1993) 201–214.
- [73] B. Neppolian, H.C. Choi, S. Sakthivel, B. Arabindoo, V. Murugesan, Solar light induced and TiO₂ assisted degradation of textile dye reactive blue 4, *Chemosphere* 46 (2002) 1173–1181.
- [74] G.K. Sarma, S. Sen Gupta, K.G. Bhattacharyya, Methylene Blue adsorption on natural and modified clays, *Sep. Sci. Technol.* 46 (2011) 1602–1614.
- [75] J. Grzechulska, A.W. Morawski, Photocatalytic decomposition of azo-dye acid black 1 in water over modified titanium dioxide, *Appl. Catal., B* 36 (2002) 45–51.
- [76] M. Sleiman, D. Vildoza, C. Ferronato, J.M. Chovelon, Photocatalytic degradation of azo dye Metanil Yellow: Optimization and kinetic modeling using a chemometric approach, *Appl. Catal., B* 77 (2007) 1–11.
- [77] E. Bulut, M. Özacar, I.A. Sengil, Equilibrium and kinetic data and process design for adsorption of Congo Red onto bentonite, *J. Hazard. Mater.* 154 (2008) 613–622.

- [78] U.G. Akpan, B.H. Hameed, Parameters affecting the photocatalytic degradation of dyes using TiO₂-based photocatalysts: A review, *J. Hazard. Mater.* 170 (2009) 520–529.
- [79] S. Lagergren, Zur theorie der sogenannten adsorption gelöster stoffe [About the theory of so-called adsorption of soluble substances], *Kungliga Svenska Vetenskapsakademiens, Handlingar*, Band 24(4) (1898) 1–39.
- [80] Y.S. Ho, Citation review of Lagergren kinetic rate equation on adsorption reactions, *Scientometrics* 59 (2004) 171–177.
- [81] I. Langmuir, The adsorption of gases on plane surfaces of glass, mica, and platinum, *J. Am. Chem. Soc.* 40 (1918) 1361–1403.